Atmos. Chem. Phys. Discuss., 9, 1301–1328, 2009
www.atmos-chem-phys-discuss.net/9/1301/2009/

Atmospheric Chemistry and Physics Discussions

This discussion paper is/has been under review for the journal *Atmospheric Chemistry and Physics (ACP)*. Please refer to the corresponding final paper in *ACP* if available.

Technical Note: In-situ quantification of aerosol sources and sinks over regional geographical scales

G. Buzorius

Meteorology department, Naval Postgraduate School, Monterey, USA

Received: 27 August 2008 – Accepted: 31 October 2008 – Published: 15 January 2009

Correspondence to: G. Buzorius (gbuzoriu@nps.edu)

Published by Copernicus Publications on behalf of the European Geosciences Union.

Abstract

In order to obtain the source/sink functions for atmospheric particulates located on the planetary surface or elevated in the atmosphere; direct aerosol emission measurements are required. For this purpose, the performance of an airborne aerosol flux measurement system with an improved 3-km spatial resolution is evaluated in this study. Eddy covariance method was used in flux calculations. A footprint for airborne flux sampling with the increased resolution becomes comparable in area to the footprint for tower sampling (with the footprint length being 2 to 10 km). The improvement in spatial resolution allows quantification of emission rates from individual sources located several kilometers apart. Locally measured aerosol flux provides useful information about aerosol sources and sinks located below or aloft of measurement altitude. The advantage is a moving platform that allows scanning of aerosol emissions or depositions over practically unlimited geographic scales. The technique delivers effective emission rates of atmospheric particulates from specific sources such as highway segments, city blocks, and remote and industrial areas. The improved spatial resolution airborne flux measurements were conducted in ambient conditions with low (<500 m) mixed boundary layer heights. Measurement results are reported from clean and partly polluted marine environments, and heavily polluted continental environments. The upward and downward fluxes from the clean marine environment were smaller than 0.5×10^6 particles $m^{-2}\,s^{-1}$ in absolute value. The effective emissions measured from a ship plume ranged from 2×10^8 to $3\times10^8\,m^{-2}\,s^{-1}$, and effective fluxes measured crossing cities plumes with populations of 10 000 to 12 000 inhabitants were in the range of 2×10^8 to $3\times10^8\,m^{-2}\,s^{-1}$. Correlations between heat and aerosol fluxes are evaluated.

1 Introduction

An amount of solar energy reaching planetary surface effectively depends on particles suspended in the atmosphere. Aerosol affects the climate directly by reflecting solar

ACPD

9, 1301–1328, 2009

radiation back into space; or indirectly, by forming cloud droplets that then reflect solar energy. Additionally, black carbon particles are able to absorb electromagnetic radiation, effectively trapping heat. An overall impact of the atmospheric aerosol has not yet been fully understood. IPCC (2001, 2007) reports pointed out that the largest uncertainties in understanding global anthropogenic climate change are in quantifying the direct and indirect climate effects caused by aerosol.

Satellite observations reported changes in marine cloud albedo caused by natural marine aerosol sources (Falkowski et al., 1992). Clouds in a continental environment increased their reflectivity after absorbing pollution plumes emitted from urban or industrial environments (Rosenfeld, 2000). Several field studies (ICARTT, 2004; MACE, 2005; and VOCALS, 2008) have been dedicated to parameterize indirect aerosol climate effects. One of the challenges in such studies is to determine the aerosol source function perturbing the cloud. Frequently, the amount of particulates entering a cloud is estimated indirectly (for example: by using vertical wind speed variance and aerosol data from flights just below the cloud base) without differentiation between the downdraft and the updraft eddies. More accurate methods differentiate between updraft and downdraft eddies.

For the quantification of aerosol sources the most direct micro-meteorological tool, the Eddy Correlation (EC) method, has been applied in other field experiments. Using the EC method, aerosol emission/deposition parameterizations were derived (for example Nilsson et al., 2001; Dorsey et al., 2002). In those studies, sampling was conducted from towers and data represented a few square kilometers of surface area (footprint). Sources that can be quantified with the EC include two major natural aerosol sources: sea spray (Pierce and Adams, 2006) and dust from arid and semi-arid areas, and probably the largest anthropogenic source: traffic. Presently, extrapolation of such data from local scale (waves, eddies and vehicles/roads) to regional or global scales involves considerable uncertainties. This extrapolation is required in order to incorporate the emission/deposition parameterizations into regional climate models.

To derive aerosol emission/deposition parameterizations over an area larger than

ACPD
9, 1301–1328, 2009

several square kilometers, a network of measurement towers or sampling from an airplane is required. In a previous study (Buzorius et al., 2006, herein referred to as "the previous paper") aerosol flux measurements from an airplane were reported. Fluxes were derived with a 10-km spatial resolution. Raw data was sampled from an airplane flying at a 50 m/s velocity. The airborne aerosol flux measurement system allows mapping of aerosol sinks and sources over a distance of hundreds kilometers.

This paper reports improvements of the spatial resolution in measuring airborne aerosol flux by using a 3-km data segment for the covariance estimate, and provides examples of the performance in various environments. The better resolution allows for more precise mapping of aerosol sources and sinks on the planetary surface. Potentially, the enhanced spatial resolution allows for a direct comparison between the tower and the airborne flux measurement systems since footprints are comparable in size. Use of a tower was not available during this study. In this paper case studies are reported when local fluxes were controlled by the vertical mixing of air mass from the flown altitude with those from atmospheric layers aloft. Deploying a mobile platform provides a possibility not only for traditional surface flux studies (such as dry deposition or surface source functions measurements) but also gives a tool for measuring aerosol uptake to the aloft layers, potentially for uptake by a cloud in cloud-aerosol interaction studies.

To evaluate EC measurements with the increased spatial resolution, the local aerosol flux data will be examined from the perspective of natural physical system behavior, considering possible aerosol ambient sinks and sources located above or below the flown altitude, and correlating the aerosol fluxes with heat fluxes, and focusing on physical processes controlling both fluxes. Presented data were sampled in areas with various mixes of natural and polluted air masses ranging from clean marine to polluted continental environments. The effective ship's emission impacts in comparison to the clean marine environment will be evaluated. The effective city emissions to the continental environment will be quantified.

ACPD
9, 1301–1328, 2009

2 Experiment setup

Experimental instrumentation deployed in this study was practically the same as reported in the previous paper but with the replacement of IRGA by LICOR 6262, for measuring water vapor concentration. A brief summary of the setup is presented here.

For fast 3-D wind speed sampling a radome system was deployed in parallel with inertial navigational system (INS) and global positioning system (GPS) (Brown et al., 1983; Tjernsrtom and Friehe, 1991). The random error in measuring wind speed after data post processing is expected to be 0.1 m s^{-1} (Buzorius et al., 2006). For total particle number concentration measurements a modified condensation particle counter model TSI 3010 was deployed. During the modification the sample flow rate was increased to 2.35 lpm, and the temperature difference between the condenser and saturator was increased to 23°C. The minimal detectable particle size with 50% efficiency after the modification was 12 nm (Buzorius, 2001). The sample inlet was just below the radome. Aerosol was sampled via 1 m long 4 mm inner diameter conductive tubing (TSI Inc. part # 3001788) at 7.5 lpm flow rate to maintain near to turbulent flow regime. Additional instruments were Heitronics KT19.85 infrared thermometer and dew point hygrometer for the sea surface temperature and dew point measurements. Air temperature was measured with a Rosemount platinum resistance thermometer. CPC data was recorded at 10 Hz, all other data at 100 Hz and during the post processing averaged to 10 Hz. CIRPAS Twin Otter aircraft was used as a measurement platform.

Data in the marine environment were collected during the Adaptive Sampling and Prediction (ASAP) experiment, in August of 2006. The sampling area for this paper was over the Pacific Ocean, off the coast of California, partially overlapping and shifted north compared to the area reported in the previous paper. Level legs were sampled at approximately 33 m in elevation.

Data collected over the continent were collected from the test flight conducted over the Salinas Valley on 3 December 2003, flying southeast of Salinas between −121.4735° longitude 36.5069° latitude and −120.9934° longitude 36.0614° latitude

ACPD
9, 1301–1328, 2009

in almost a straight line about 66 km long. Level legs were sampled at approximately 180 m in elevation as determined by the airplane's radar.

3 Methodology

3.1 Eddy-Correlation (EC)

Aerosol flux (F) is determined through a covariance formula, as shown in Eq. (1) below,

$$F = \overline{w'c'}, \quad (1)$$

where the prime denotes a deviation from the mean value; the over bar means an average over the 200 or 60 s time period; w is the vertical wind speed in m/s; $w'=w-\overline{w}$; c is the aerosol number concentration in m^{-3}; and $c'=c-\overline{c}$. The linear de-trending filter was applied to the time series to remove linear trends prior to the calculating fluxes.

The flux uncertainties are due to the error in measuring vertical wind speed, limited counting statistics, and limited Condensation Particle Counter (CPC) response time. Each of the first two sources leads to an approximately 0.1×10^6 particles $m^{-2}\,s^{-1}$ flux error individually when the aerosol number concentration is about 10^3 particles cm^{-3} (Buzorius et al., 2006). Those errors are random and therefore can be reduced by increasing the time window in the flux formula, or by repeating measurements in the same sampling area. A more detailed discussion of the measurement errors was reported in the previous paper. The "Webb correction" will be presented further in this paper.

3.2 Footprint

The sea surface fetch contributing to the flux is defined as a footprint. There is a distance from the sampling point towards the upwind direction within the footprint, at which the contribution peaks and decays faster towards the sampling tower and comparably slower towards the upwind direction. The peak is sharper and the footprint

area is smaller during the unstable atmospheric conditions and over the rough surfaces. Leclerc and Thurstell (1990) estimated that 90% of the flux is caused by processes at the surface area extending 0.1 to 8 km from the tower towards the upwind direction, when the sampling altitude is 30 m during the neutral stratification and the roughness length being 6 millimeters (mm). For a roughness length of 0.6 mm (in the marine case study, the roughness length was found to be from 0.1 to 2.5 mm) the peak distance is about 800 m. Other footprint models for similar environmental conditions suggested a peak distance of 1 to 2 km and a 90% flux distance of 3 to 6 km (http://footprint.kljun.net/contact.php). The footprint for airborne sampling is going to be somewhat skewed along the airplane track. It is a different shape for airplanes flying along the wind direction and in perpendicular alignment. Yet, a more detailed study on the footprint, while sampling from an aircraft, is out of the scope of this paper.

3.3 Webb correction

Webb et al. (1980) pointed out that measured concentration fluxes of the atmospheric constituent can be affected by heat or water vapor fluxes. The reasoning was that for the heat flux being directed upwards, an air parcel rising towards the sampling point has a slightly higher temperature and therefore, a slightly lower air density compared to the descending air parcel. Assuming a constant aerosol concentration at different altitudes and zero particle vertical transport the density fluctuation due to the differences in temperature between the descending and ascending parcels results in fluctuating air volume for a constant particle number at the sampling point. Moreover, this fluctuation is correlated with the vertical wind speed, and manifests as an artificial particle flux as measured by eddy correlation. The same thing occurs due to the water vapor flux since partial vapor pressure is a component in the air parcel total pressure. The particle flux components due to the sensible or latent heat fluxes are proportional to the sensible or latent heat fluxes and aerosol concentration. Total particle flux, as shown below in

Eq. (2), is:

$$F = \overline{w'c'} + 1.61\frac{\overline{c}}{\rho_a}\overline{w'\rho_v} + (1 + 1.61\overline{q})\frac{\overline{w'T'}}{\overline{T}}\overline{c} \quad (2)$$

where T is the absolute temperature; ρ_a is the density of dry air; ρ_v is the density of water vapor; and q with over-bar is the averaged specific humidity. Both corrections are significant when the covariance of aerosol and vertical wind speed is low and the sensible and latent heat fluxes are high.

3.4 Spatial resolution

In order for the covariance estimate (Eq. 1) to be representative of the vertical flux, a sampling of the full size range of atmospheric eddies is required. The range defines the length of time series (in the time space for tower measurements and the distance space for airborne studies) of two atmospheric scalars that are required in the covariance formula. Typically, the length is defined using a cumulative sum (Ogive) or co-spectrum analysis.

A comparison reported in the previous paper (Fig. 6, Buzorius et al., 2006) between the airborne heat flux calculated for every 5-km segment and the heat flux derived using the bulk method (COARE 3.0) showed a general agreement. It was concluded in the previous paper that 5-km segments were long enough to capture the full range of eddy sizes.

Figure 1 shows a comparison between heat fluxes derived using EC over 5-km and 3-km segments. The data were collected in the marine environment during an 8 August 2006 flight. The variability in the heat flux was caused by a drop in the sea surface temperature due to the cold water upwelling in coastal waters. The fragment of the flight is presented where the airplane flew in and out of the area with the lower SST. The 3-km segment heat flux shows the slightly steeper changes compared to the 5-km segment fluxes, because the later uses longer averages. Overall, both flux series tracked well the changes in the heat flux. As shown in the previous paper, with the 5-km segment

ACPD
9, 1301–1328, 2009

fluxes resembling values of the bulk estimates, and the 3-km segment fluxes having very similar values compared to the 5-km segment fluxes, it can be safely assumed that the 3-km segments have sufficiently long series to capture the full range of the eddy size spectrum. The heat flux is primarily driven by heat exchange between the sea surface and the atmosphere. It is safe to assume that a flux of another atmospheric constituent (i.e., aerosol concentration), that is primarily driven by material exchange across the ocean-atmosphere interface, will be sufficiently represented by a 3-km segment covariance.

Aerosol concentration power spectrum from "Fast-Fourier-Transformation" or "Ogive" analyses are more direct methods in verifying the minimum length of the data stream required in the covariance equation. However, the aerosol concentration in the coastal environment was frequently increased tenfold by human-caused sources. If a 3-km segment was of the clean marine aerosol with total number below 1000 particles cm^{-3}, extending that segment to 5- or 10-km, frequently lead to the incorporation of anthropogenic aerosol plumes from ships or continental polluted air encountered by the airplane further into the flight. The Ogive (spectrum) analysis was frequently corrupted by such plumes.

Mixed Boundary Layer (MBL) height defines the dominant atmospheric eddy sizes. In this paper, it was adopted that the segment length used in Eqs. (1) and (2) has to be several times longer than the MBL height (see also Businger, 1986). Below, the results will be presented from comparisons between the 3-km and the 10-km segment aerosol fluxes sampled in various environments.

4 Results and discussion

Calculated aerosol fluxes included all of the above-mentioned corrections. The Webb correction in the marine environment was less than 3% in 70% flux data points and was less than 5% in 80% of data. In the continental environment the correction was less than 2%.

ACPD
9, 1301–1328, 2009

Presented here are locally (approximately at 33 m elevation) measured fluxes. Direct comparison between the local flux and the surface flux is impossible because the later was not available. Theoretically, the total aerosol number flux divergence between the surface and the measurement elevation occurs due to coagulation, the process that over a time reduces total aerosol number concentration. However, if the coagulation occurs on the same rate in updraft and downdraft air parcels, then the EC value is not affected by the coagulation. Additionally, coagulation is negligible in clean marine environment with low wind speeds over a time period comparable to characteristic atmospheric time scales. The main interest in this study is the experimental determination of aerosol local flux in various environments. Examples below illustrate situations when local fluxes are dominated by exchange across planetary surface-atmosphere interface or by dilution with atmospheric layers aloft.

4.1 Single plume in a clean environment

In the sampling area during the ASAP experiment, the marine aerosol was superimposed with particles emitted from ships. Figure 2 presents an example of the 10-km and the 3-km segment aerosol fluxes while the airplane crossed a pollution plume from a ship. Particle concentration plotted on the right-y axis shows an increase from 500 particles cm^{-3} outside the plume to 11 000 particles cm^{-3} inside the plume. The width of the spike at the half height was 3 s (150 m). This plume was encountered on the 12 August 2006 flight. On that day measured wind speeds were 1 to 3 m/s at a 33 m elevation. Very calm weather that day lead to the slow plume dispersion. Almost a delta-function behavior in the concentration time series provided a good example for demonstrating the differences between the 10-km and the 3-km segment fluxes (dotted and dashed lines).

EC method requires a horizontal homogeneity in scalar concentration. The requirement is not satisfied after the plume levels-off and causes spatial non-homogeneity in aerosol concentration. In non-homogeneous environment the direction of EC flux fluctuate significantly because an increase in aerosol number from the mean value

ACPD
9, 1301–1328, 2009

coincides randomly with the vertical wind speed direction and the fluxes have the relatively large absolute values. In the presented example it is assumed that the airplane encountered a plume in the relatively early stage, before the leveling-off. The assumption is supported by the short cross-sectional plume distance (150 m) that indicated of the relatively short horizontal distance from the ship, and consistently upward fluxes.

The fluxes outside the plume were below 10^6 particles $m^{-2}\,s^{-1}$. When the plume was encountered, the 10-km segment flux increased to about 15×10^6 particles $m^{-2}\,s^{-1}$ and the 3-km segment flux jumped to a 50×10^6 to 70×10^6 particles $m^{-2}\,s^{-1}$ range. An integral area under the flux curve (not the curve maximal values) represents the effective source strength. The integral area under the 3-km flux curve is about 15% larger compared to the area under the 10-km flux curve. The increase in the spatial resolution from 10-km to 3-km allows for more precise source localizations, which becomes valuable when several sources are present.

4.2 Multiple plumes

When multiple plumes are present the averaged aerosol concentration over 3-km distance increases significantly compared to the clean environment. The increase causes a reduction in value of $c'=c-\overline{c}$ and, the relative fluctuations in aerosol concentration can satisfy EC spatial homogeneity requirement (Dorsey et al., 2002; Mårtensson, et al., 2006).

On the 8 August 2006 flight, a total four large ships were present in the sampling area. This flight provided an example of the overlapping of several plumes in a clean marine environment. One of the ships, a Hyundai containership, was visually observed several times from the airplane, while the other three were detected by the airplane's radar. During the flight fragment that was the closest to the shoreline, a continental aerosol was mixed-in with the marine aerosol. Figure 3 demonstrates the wind patterns on that day. Wind direction was from the northwest, which is typical for the area. Wind speeds varied from 8 to 10 m/s outside the bay, and subsided to less than 4 m/s inside the bay due to air flow expansion downwind of the cape. Virtual potential temperature

ACPD
9, 1301–1328, 2009

vertical soundings showed a homogeneous mix between the surface and 300 to 400 m in elevation at offshore locations. The sounding sampled close to the shoreline inside the bay showed a decoupling at 220 m in altitude where the temperature increased, due to outflow of the warmer continental air. Figure 4 illustrates aerosol number concentrations measured at 33 m elevation during that flight. In areas with clean marine air masses aerosol number concentrations varied from 300 to 800 particles cm^{-3}. In the ship's plume aerosol number increased to 10^4 to 2×10^4 particles cm^{-3}. The single spike at about -122.45° longitude and 36.8° latitude was from the Hyundai containership when it was visually observed from the airplane for the first time. Multiply spikes at -122.6° longitude and 36.9 to 37.2° latitude are from several plumes. Approaching the coastline, the continental pollution increased the aerosol number concentration to about 9000 particles cm^{-3}.

In Figs. 5 and 6 aerosol fluxes were calculated using the 10-km and the 3-km segments. Differences between the figures demonstrate the improved spatial resolution. For example, a small area in red marks the single concentration spike at -122.45° longitude and 36.8° latitude (Fig. 6). While Fig. 5 shows strong upward fluxes in the unrealistically larger area compared to the corresponding spike in concentration data from Fig. 4. Both figures use averages over $0.035^\circ\times0.035^\circ$ cells. Multiple plumes in the northern part mainly caused strong upward fluxes. Strong downward fluxes adjacent to the upward fluxes in the plume were also observed. Those were caused by the plume aerosol deposition to the ocean surface and random errors in measuring turbulence (see blue patches close to plumes) or errors due to non-homogeneity in aerosol concentration. Figure 6 presents more precise locations than Fig. 5 of the emission sources referenced to the spikes in concentration data from Fig. 4. Aerosol flux maximal values in ship plumes were reaching $3\times10^8\ m^{-2}\ s^{-1}$. The range of color scale in both figures was reduced for a visually better representation of the variability in flux direction (dark red marks fluxes larger than $30\times10^6\ m^{-2}\ s^{-1}$). Additional reduction in the flux amplitude in both figures was due to spatial averaging across 0.035×0.035 degrees of longitude and latitude cells.

ACPD
9, 1301–1328, 2009

Inside the bay a pollution plume from the City of Santa Cruz was observed. The increase in aerosol number concurred with the upward fluxes, due to the aerosol dilution aloft of the measurement altitude that was confirmed from vertical profile data (not pictured). On the western side of the plume, downward fluxes were observed. The sea surface was acting as a net aerosol sink due to the dry deposition of plume particles (Slinn and Slinn, 1980; Sievering, 1981). A relatively high aerosol number (~9000 particles cm^{-3}) in the continental plume yielded to strong downward fluxes (-10^7 to $-15\times10^6\,m^{-2}\,s^{-1}$). This behavior (upward flux in the continental plume and the downward flux from the west side) was observed during other flights as well, when winds brought continental pollution to the marine environment.

Effective flux measured from transect of a single ship plume was measured up to 3×10^8 particles $m^{-2}\,s^{-1}$. A fraction of the emitted particles with dominant sizes in the Aitken mode are able to act as cloud condensation nuclei (CCN). Ship emissions mixed into marine clouds are able to reduce the cloud droplet effective radius and to increase the cloud albedo (Hobbs et al., 2000). Exact parameterizations linking the aerosol source strength and the change in the albedo are very scarce in scientific literature, partly due to the lack of flux measurements. Direct measurements of CCN flux are not available because CCN counters do not satisfy EC requirements. When other significant aerosol sink/sources are not present, the CCN flux can be preliminary estimated indirectly by determining a fraction of CCN within the total aerosol number concentration and projecting that fraction to the total aerosol number flux.

4.3 Aerosol fluxes in a clean marine environment

In a clean marine environment, local fluxes measured at approximately 33 m altitude represent an overall sum of forces causing upward and downward directed aerosol transports. Forces are caused mainly from the aerosol generation and removal processes, acting independently of each other. The aerosol generation is caused by bubble bursting during breaking waves. Atmospheric turbulence carries particles from the ocean-atmosphere interface to higher elevations and mixes them through the entire

ACPD
9, 1301–1328, 2009

mixed boundary layer column with typical height being from 100 to 500 m. Aerosols are removed from the MBL by dry deposition (Slinn and Slinn, 1980), entrainment aloft of the mixed boundary layer, coagulation (reduces the number, not the mass) and some particles can be activated into cloud droplets. Measured aerosol number concentration varied from 300 to 800 particles cm^{-3}. Similar values were reported in other sites from clean marine environment (Bates et al., 2000). Vertical soundings sampled during spirals indicated a homogeneous mix of aerosol number in MBL in clean marine environment. In the steady state situation where the upward and the downward fluxes are equal, the total sum of fluxes (measured flux) approaches zero. Observed in this study, aerosol fluxes in the clean marine environment on average were consistently within the range -0.5 to $+0.5\times10^{6}$ particles $m^{-2}\,s^{-1}$. During this flight the wind speed was not strong enough (less than 8 m/s at nominal 10 m elevation) to cause significant sea-spray emissions. Measured upward fluxes ranges similarly with the data from other sites (Nilsson et al., 2001; O'Dowd and de Leeuw, 2007). Using the fitted data from the Arctic Ocean sea spray flux measurements a value of $0.62\times10^{6}\,m^{-2}\,s^{-1}$ during 8 m/s horizontal wind at the nominal height was reported.

Experimental data from various field campaigns suggest a factor of 2 in the sea spray source function variability for the given wind speed (Clarke et al., 2006). Water temperature has been identified as one of the variables modifying the function (Mårtensson et al., 2003), while other factors are still subject of research (Lewis and Schwartz, 2004). Recently, dissolved organic materials have been identified as a possible primary marine aerosol source (Tyree et al., 2007; O'Dowd and DeLeeuw, 2007; Nilsson et al., 2007). Using an airplane as a measurement platform it is possible to measure the aerosol flux over two marine areas that are different only by one physical or chemical property but otherwise are identical. Within the sampling area during the AOSN and ASAP experiments ocean surface pools with the increased chlorophyll concentrations were observed using a remote sensing spectroscopic instrument installed on the airplane (not presented here). Unfortunately, data analysis showed significant ship emissions in areas with the chlorophyll pools during AOSN field campaign and unusu-

ally low wind speeds (minimal white cap areas) during the ASAP experiment in 2006. Due to these reasons this study's dataset could not be used for detecting the upward natural marine aerosol flux enhancement over the chlorophyll pools. The flux increase would be expected if there was a primary source of pure (not containing NaCl) organic carbon aerosols.

4.4 Polluted environment

Data above the land were collected while flying in the Salinas Valley, inland from the marine example. West of −121.1° longitude the airplane's track was very close to Highway 101. East of the longitude the track shifted south of the highway and was mainly over the agricultural fields and vineyards. The highway in the sample area is surrounded by agricultural fields. The Cities of Soledad, Greenfield and King City are along the highway with populations of 11 300, 12 600 and 11 000, respectively (US Census, 2000). The valley itself is surrounded by mountains at distances from the track longer than footprint estimates (90% flux was contributed from 10 km long fetch). Vertical soundings indicated a mixed boundary layer up to the 470 m elevation where virtual potential temperature decoupled. It is recognized that large eddies formed by the air motion over the hills and the valley might affect the measured flux. However, a more detailed analysis of large eddies is out of scope for this paper.

Heat flux in the continental environment is mainly driven by a warmer air rising from the surface, where the surface is heated by solar radiation. Simultaneously, the surface in the continental environment can act as a net aerosol sink via the particle dry deposition mechanism (Lamaud et al., 1994; Slinn, 1982); or as a net aerosol source for coarse particle re-suspension or submicron and ultrafine aerosol emissions from traffic (Dorsey et al., 2001; Mårtensson et al., 2006). The re-suspension can be neglected here since the total aerosol number is dominated by smaller particles than the coarse mode. Depending on whether the surface is the net aerosol sink or source, the aerosol flux will have a negative or a positive correlation with the heat flux.

Figure 7 presents the aerosol concentration in the bottom panel, the aerosol and

ACPD
9, 1301–1328, 2009

the heat fluxes in the corresponding top panel left-y and right-y axes, sampled above the land. The plot presents data collected over the 66-km long study area. The aerosol number concentration was sampled at 10 Hz. At longitudes −121.4°, −121.31°, −121.195° and −121.04° to −121.02° the aerosol (solid line) and the heat fluxes (dotted line) are negatively correlated (an increase in the heat flux concurs with the lowest aerosol fluxes and vice versa).

At −121.4° and −121.31° longitude, the positive aerosol flux concurs with a very high ~25 000 cm^{-3} aerosol number and the downward heat flux. It is atypical to observe, although small (~−2 to −5 $W m^{-2}$) but downward heat flux during daylight above land. Most likely, the air masses at 180 m elevation west of −121.3° longitude did not represent properties of the air masses close to the surface. The plotted data suggests the mixing between the polluted air from the valley and the warmer air from aloft. The virtual potential temperature jumped from 292 to 294 K aloft of a 470 m elevation. Concurrently, the aerosol number concentration was reduced by about 50% above the 470 m elevation. The mixing of such air masses resulted in the strong upward aerosol and the downward heat fluxes. In these episodes the measured aerosol flux represented an uptake of particles due to dilution aloft of the measurement elevation.

At longitudes −121.195° and −121.04° to −121.02° the aerosol concentration drops to 3000 to 5000 particles cm^{-3}, typical values for a remote continental environment. Simultaneously, the heat flux increases to 30 to 40 $W m^{-2}$ range and the aerosol flux is downwards fluctuating between 0 to -200×10^{6} particles $m^{-2} s^{-1}$. The relatively low aerosol number concurrent with the increase in the upward heat flux, and the downward aerosol flux are characteristics of the air mass coming from low elevations, close to the planetary surface. The upward heat flux was caused by the heat transfer from the planetary surface warmed-up by solar radiation. The downward aerosol flux was caused by the surface acting as an aerosol sink via the dry deposition mechanism. The heat and aerosol transfer across the interface between the planetary surface and the atmosphere explains the observations for the given longitude segments.

Numerous anthropogenic aerosol sources such as highway and local traffic, agricul-

tural activities, and advection caused non-homogeneity in aerosol concentration time series. Pollution plumes were overlapped, and tracing each of them to the specific source was impossible for all but a couple major plumes.

Using the wind direction data and Google Earth mapping techniques, the aerosol concentration increases at −121.31° and −121.22° longitude in Fig. 7 bottom panel are attributed to emissions from Soledad and Greenfield with the corresponding upward aerosol fluxes in top panel. Similar measurements from the City of Stockholm, Sweden (population 750 000) showed fluxes (Mårtensson et al., 2006) reaching a $\sim 2\times10^9$ to 3×10^9 particles $m^{-2}\,s^{-1}$ range, while in this study urban fluxes were as high as $\sim 3\times10^8$ particles $m^{-2}\,s^{-1}$. The emissions were driven by traffic and comparably the smaller traffic intensity from the smaller cities leads to the lower emission rates. Note that the aerosol concentration in the Soledad and Greenfield plumes and the Stockholm tower measurements are in the same range reaching 25 000 particles cm^{-3} (the upper limit for identical instruments used in both projects), yet the fluxes differ by an order of magnitude. The aerosol concentration in addition to the traffic intensity depends on the MBL height and aerosol population dynamics.

5 Conclusions and summary

This work reports airborne aerosol flux measurements with an improved spatial resolution to 3-km segments. The 3-km distance corresponds to about a minimal footprint length when fluxes are sampled from towers. This study increases the range of applications of eddy correlation method for estimating aerosol emission sources/sinks on planetary surface and provides a better utilization of data collected from an aircraft. The presented method is particularly useful when the effective fluxes have to be measured during the relatively short time period to assure the same meteorological conditions over a wide distance: estimating aerosol source strengths for various city grids, industrial areas, ocean surfaces varying by one parameter while other (for example horizontal wind speed, water temperature) are identical. An alternative is deployment

ACPD
9, 1301–1328, 2009

of EC towers network that is not necessarily cost affective and sometimes impossible. Caution must be exercised limiting the application to ambient conditions where the 3-km segment length is several times longer compared to the height of mixed boundary layer height.

The measured local aerosol emission rates from the clean marine environment were smaller than $0.5\times10^{6}\,m^{-2}\,s^{-1}$ during the low horizontal wind speeds conditions. Positive values of the measured natural marine aerosol flux were similar to those reported in other sites. The effective emissions from ship plumes and cities (populations of 10 000–12 000) were in the range of a 2×10^{8} to 3×10^{8} particles $m^{-2}\,s^{-1}$. The ocean surface acted as a sink for marine and continental aerosols with removal rate of $-0.5\times10^{6}\,m^{-2}\,s^{-1}$ and $-10^{7}\,m^{-2}\,s^{-1}$ to $-15\times10^{6}\,m^{-2}\,s^{-1}$, respectively (a minus sign indicates the downward flux). The flux correction due to the air density fluctuations were smaller than 2% in the continental environment, and smaller than 5% in 80% data points in the marine environment. A high potential of this dataset was to compare the natural marine aerosol emission flux from the ocean surface area with the chlorophyll pool to the flux outside the pool, while all other environmental parameters are identical. However, low wind speeds (less than 8 m/s at 33 m elevation for the majority of flights) during ASAP field campaign in 2006 significantly limited white cape areas (no breaking waves), and reduced the release of particulates from the ocean to the atmosphere via the bubble burst mechanism and no significant difference in the fluxes between areas were observed.

Aerosol flux from urban areas primarily was upwards with traffic being one of the main particle sources. Outside the urban plume, aerosol fluxes were found to be downwards or upward: when the planetary surface was acting as a net aerosol sink; or represented a mixing with the relatively cleaner air masses aloft (dilution of aerosol concentration). A vertical aerosol concentration profile or a reference to the heat flux direction is required in interpreting the aerosol local flux data collected from the single altitude. The technique provides a unique tool for aerosol source and sink quantifications over unlimited geographical scales with a spatial resolution of 3-km. Additionally

ACPD
9, 1301–1328, 2009

the technique is suitable for measurement of aerosol transport to layers aloft – a useful tool in cloud-aerosol interaction studies. Such data is urgently required for parameterizations of aerosol climatic effects and in regional climate models. Further research is required for the better understanding of the link between the local and surface fluxes, aerosol flux divergence, and footprint for airborne sampling.

Acknowledgements. This study was supported by NSF SGER grant #0634147. Author is thankful to S. Ramp from NPS for accommodating aerosol flux study during the ASAP field campaign. Q. Wang and J. Kalogiros are acknowledged for sharing post-processed wind speed data. Author is grateful to N. Kljun for footprint estimates provided at website http://footprint.kljun.net/contact.php.

References

Bates, T. S., Quinn, P. K., Covert, D. S., Coffman, D. J., Johnson, J. E., and Wiedensohler, A.: Aerosol physical properties and processes in the lower boundary layer: a comparison of shipboard sub-micron data from ACE-1 and ACE-2, Tellus, 52B, 258–272, 2000.

Brown, E. N., Friehe, C. A., and Lenschow, D. H.: The use of pressure fluctuations on the nose of an aircraft for measuring air motion, J. Clim. Appl. Meteorol., 22, 171–180, 1983.

Businger, J. A.: Evaluation of the accuracy with which dry deposition can be measured with current micrometeorological techniques, J. Clim. Appl. Meteorol., 25, 1100–1124, 1986.

Buzorius, G., Kalogiros, J., and Varutbangkul, T.: Airborne aerosol flux measurements with eddy correlation above the ocean in coastal environment, J. Aerosol Sci., 37, 1267–1286, 2006.

Buzorius, G.: Cut-off sizes and time constants of the CPC TSI 3010 operating at 1 to 3 lpm flow rates, Aerosol Sci. Tech., 25, 577–585, 2001.

Clarke, A. D., Owens, S. R., and Zhou, J.: An ultrafine sea-salt flux from breaking waves: Implications for cloud condensation nuclei in remote marine atmosphere, J. Geophys. Res., 111, D06202, doi:10.1029/2005JD006565, 2006.

Dorsey, J. R., Nemitz, E., Gallagher, M. W., Fowler, D., Williams, P. I., Bower, K. N., and Beswick, K. M.: Direct measurements and parameterization of aerosol flux, concentration and emission velocity above a city, Atmos. Environ., 36, 791–800, 2002.

IPCC: Climate Change 2001, Intergovernmental Panel on Climate Change, edited by co-chairs Houghton, J. T. and Ding, Y., published by Cambridge University press, 2001.
IPCC: Climate Change 2007, Intergovernmental Panel on Climate Change, http://www.ipcc.ch, 2007.
Hobbs, P. V., Garrett, T. J., Ferek, R. J., Strader, Sc. R., Hegg, D. A., Frick, G. M., Hoppel, G. M., Gasparovic, R. F., Russell, R. F., Johnson, L. M., O'Dowd, C. D., Durkee, C., Nielsen, P. A., and Innis, K. E.: Emissions from ships with respect to their effects on clouds, J. Geophys. Res., 57, 2570–2590, 2000.
Falkowski, P. G., Kim, Y., Kolber, Z., Wilson, S., Wirick, C., and Cess, R.: Natural versus anthropogenic factors affecting low-level cloud albedo over the North Atlantic, Science, 256, 1311–1313, doi:10.1126/science.256.5061.1311, 1992.
Lamaud, E., Chapuis, A., Fontan, J., and Serie, E.: Measurements and parameterization of aerosol dry deposition in a semi-arid area, Atmos. Environ., 28, 2461–2471, 1994.
Leclerc, M. Y. and Thurtell, G. W.: Footprint predictions of scalar fluxes using a Markovian analysis, Bound.-Lay. Meteorol., 52, 247–258, 1990.
Lewis, E. R. and Schwartz, S. E.: Sea salt aerosol production: mechanisms, methods, measurements, and models, Geophys. Monogr. Ser., vol. 152, 413 pp., AGU, Washington, D.C., 2004.
Mårtensson, M., Nilsson, E. D., de Leeuw, G., Cohen, L. H., and Hansson, H.-C.: Laboratory simulations of the primary marine aerosol generated by bubble bursting, J. Geophys. Res., 108, 4297, doi:10.1029/2002JD002263, 2003.
Mårtensson, M., Nilsson, E. D., Buzorius, G., and Johansson, C.: Eddy covariance measurement and parameterization of traffic related particle emissions in an urban environment, Atmos. Chem. Phys., 6, 769–785, 2006, http://www.atmos-chem-phys.net/6/769/2006/.
Nilsson, E. D., Rannik, U., Swietlicki, E., Leck, C., Aalto, P. P., Zhou, J., and Norman, M.: Turbulent aerosol fluxes over the Arctic Ocean 2. Wind driven sources from the sea, J. Geophys. Res., 106, 32139–32154, 2001.
Nilsson, E. D., Mårtensson, E. M., Van Ekeren, J. S., de Leeuw, G., Moerman, M., and O'Dowd, C.: Primary marine aerosol emissions: size resolved eddy covariance measurements with estimates of the sea salt and organic carbon fractions, Atmos. Chem. Phys. Discuss., 7, 13345–13400, 2007, http://www.atmos-chem-phys-discuss.net/7/13345/2007/.

O'Dowd, C. D. and de Leeuw, G.: Marine aerosol production: a review of the current knowledge, Philos. T. Roy. Soc. A, 365, 1753–1774, 2007.
Pierce, J. R. and Adams, P. J.: Global evaluation of CCN formation by direct emission of sea salt and growth of ultrafine sea salt, J. Geophys. Res., 111, D06203, doi:10.1029/2005JD006186, 2006.
Rosenfeld, D.: Suppression of rain and snow by urban and industrial air pollution, Science, 287, 1793–1796, 2000.
Sievering, H.: Profile measurements of particle mass transfer at the air-water interface, Atmos. Environ., 15, 123–129, 1981.
Slin, S. A. and Slin, W. G. N.: Predictions for particle deposition on natural waters, Atmos. Environ., 16, 301–306, 1980.
Slinn, W. G. N.: Predictions for particle deposition to vegetative canopies, Atmos. Environ., 16, 1785–1794, 1982.
Tjernstrom, M. and Friehe, C. A.: Analysis of a radome air-motion system on a twin-jet aircraft for boundary-layer research, J. Atmos Ocean. Tech., 8, 19–40, 1991.
Tyree, C. A., Hellion, V. M., Alexandrova, O. A., and Allen, J. O.: Foam droplets generated from natural and artificial seawaters, J. Geophys. Res., 112, D11204, doi:10.1029/2006JD007729, 2007.
US Census 2000. http://www.census.gov.
Webb, E. K., Pearman, G. I., and Leuning, R.: Correction of flux measurements for density effects due to heat and vapor transfer, Q. J. Roy. Meteorol. Soc., 106, 85–100, 1980.

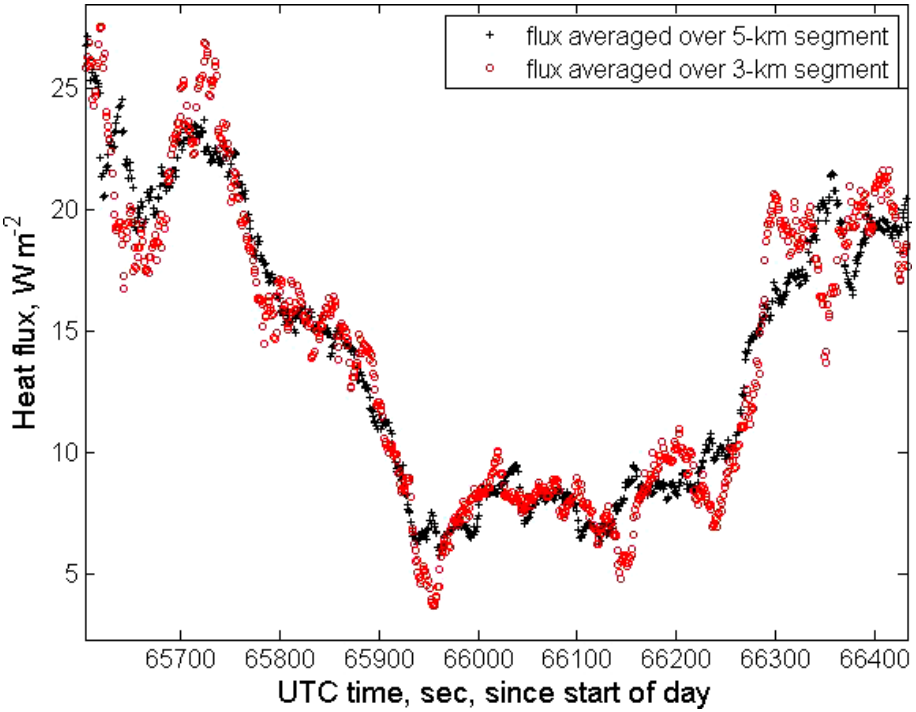

Fig. 1. Heat flux sampled at 33 m elevation above the ocean over a distance of about 40 km.

ACPD
9, 1301–1328, 2009

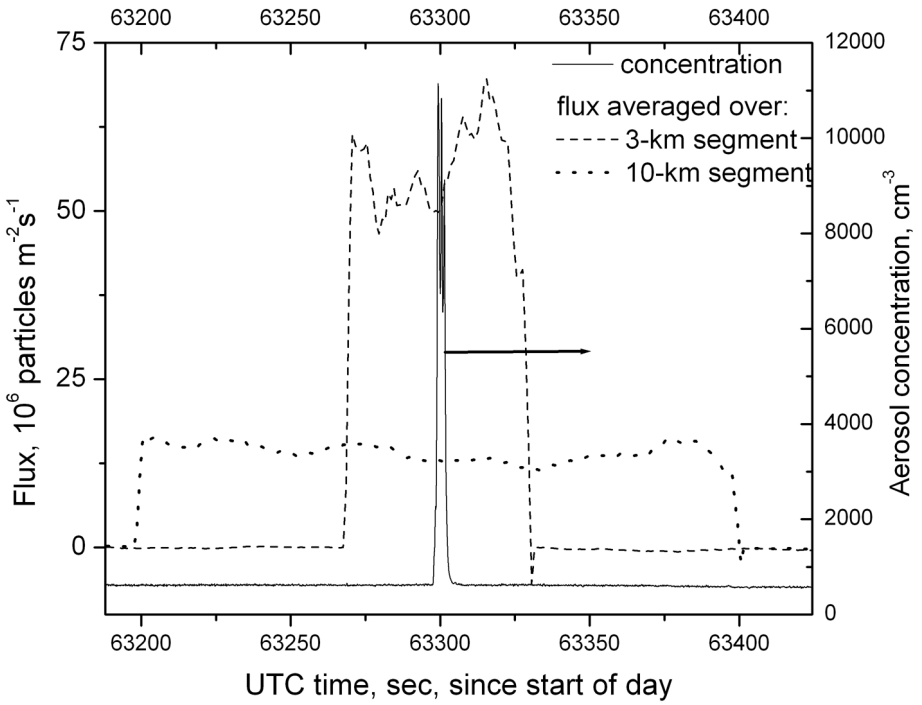

Fig. 2. A sharp rise in aerosol concentration and aerosol fluxes due to ship emissions sampled on 12 August 2006.

ACPD
9, 1301–1328, 2009

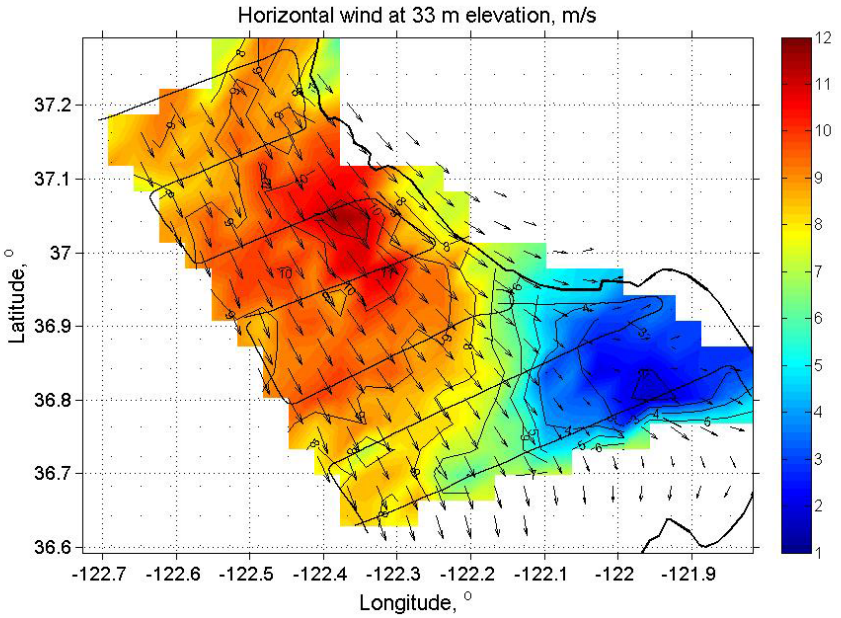

Fig. 3. Wind speed and direction distribution on 8 August 2006. Thin line indicates airplane track, thick line shows coastline.

ACPD
9, 1301–1328, 2009

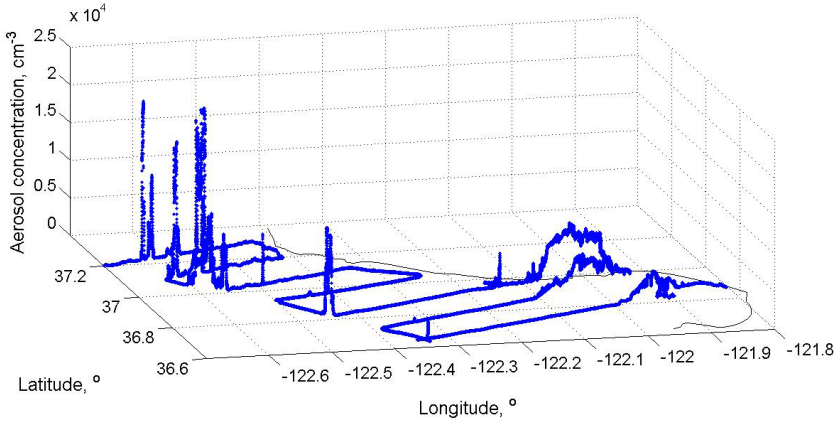

Fig. 4. Spatial distribution of total aerosol number concentration.

ACPD
9, 1301–1328, 2009

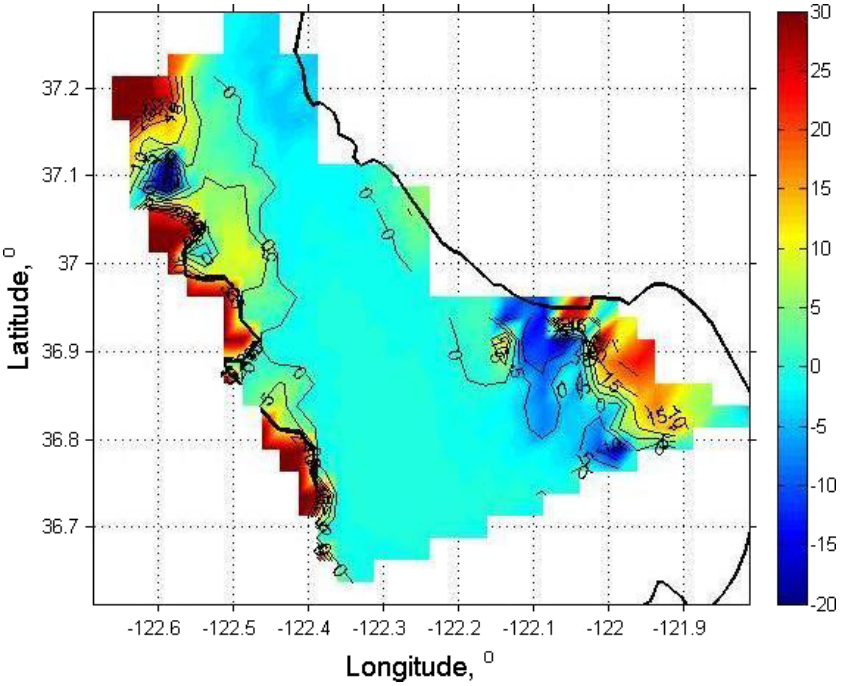

Fig. 5. Aerosol flux calculated over each 10-km segment sampled 8 August 2006. Thick line is coastline. Color scale is units of particles $10^6\,m^{-2}\,s^{-1}$.

ACPD
9, 1301–1328, 2009

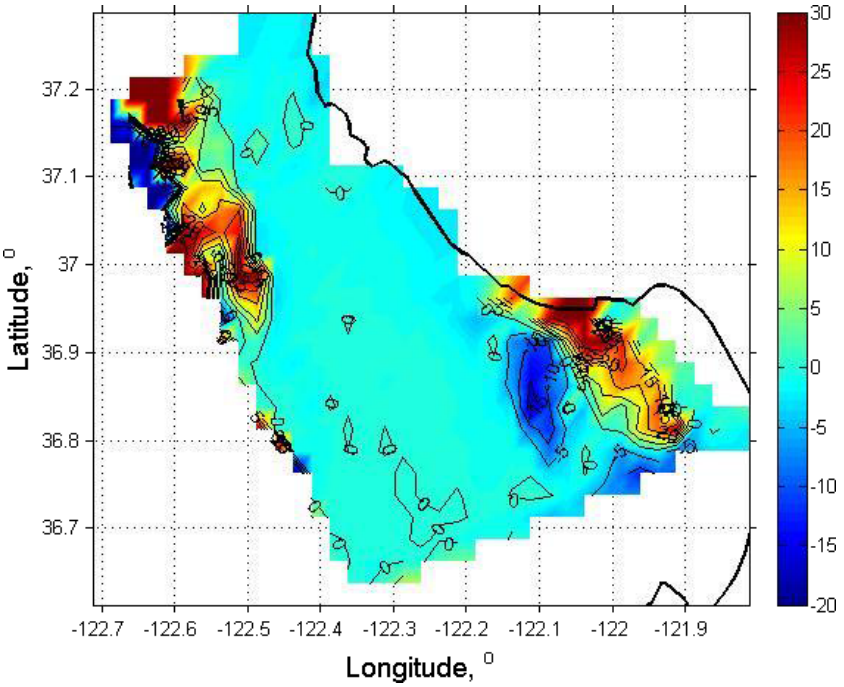

Fig. 6. Same as Fig. 5 but aerosol flux was calculated over each 3-km segment.

ACPD
9, 1301–1328, 2009

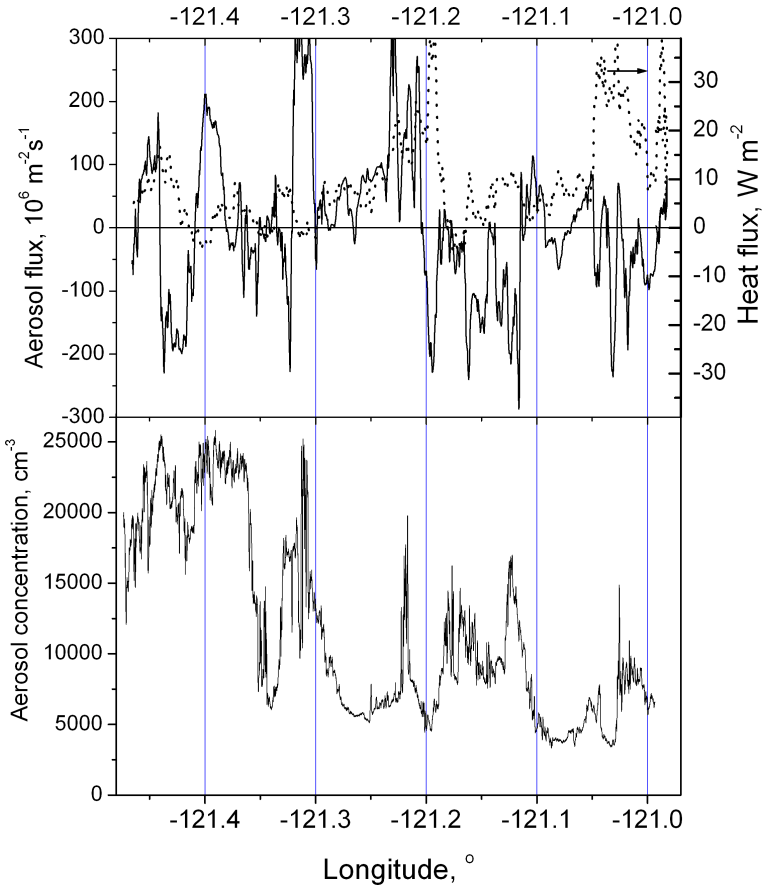

Fig. 7. Aerosol sampling across 66 km distance 180 m above the land. Bottom panel shows total aerosol number concentration (10 Hz). Top panel shows 3-km aerosol flux on the left-y axis. Heat flux is in dotted line (right-y axis).

ACPD
9, 1301–1328, 2009